

Hierarchical Statistical Characterization of Mixed-Signal Circuits Using Behavioral Modeling

Eric Felt

Stefano Zanella[†]

Carlo Guardiani^{††}

Alberto Sangiovanni-Vincentelli

Electrical Engineering and Computer Sciences
University of California, Berkeley
Berkeley, California

[†]Elettronica ed Informatica
Università degli Studi di Padova
Padova, Italy

^{††}Central R&D D.A.I.S.
SGS-Thomson Microelectronics
Agrate Brianza, Italy

Abstract

A methodology for hierarchical statistical circuit characterization which does not rely upon circuit-level Monte Carlo simulation is presented. The methodology uses principal component analysis, response surface methodology, and statistics to directly calculate the statistical distributions of higher-level parameters from the distributions of lower-level parameters. We have used the methodology to characterize a folded cascode operational amplifier and a phase-locked loop. This methodology permits the statistical characterization of large analog and mixed-signal systems, many of which are extremely time-consuming or impossible to characterize using existing methods.

1 Introduction

Statistical circuit characterization is essential for estimating yield, for designing manufacturable and robust systems, for deriving “worst-case” models, and for testing. The most widely used technique for performing statistical characterization is Monte Carlo analysis [1, 2]. Unfortunately, the accuracy of results produced by a Monte Carlo analysis is only proportional to the square root of the number of simulations performed, and the number of Monte Carlo simulations required to produce a relatively accurate result increases exponentially with the number of low-level statistical parameters. Therefore Monte Carlo techniques can be very expensive, unacceptably inaccurate, or both.

One promising approach to dealing with these shortcomings involves the use of behavioral models and *hierarchical* characterization. Hierarchical characterization is illustrated in Figure 1. This characterization method is part of a hierarchical design methodology which involves different levels of abstraction [3]. The low-level parameters typically represent transistor model parameters, such as t_{ox} and V_{T0} . The intermediate-level parameters typically represent behavioral model parameters, such as open-loop gain and offset of an operational amplifier. The high-level performances represent circuit performance specifications, such as signal-to-noise ratio of an analog-to-digital converter. A circuit simulator such as SPICE [4] is used to simulate the intermediate-level parameters as functions of the low-level parameters, and a behavioral-level simulator such as MIDAS [5] is used to simulate the high-level performances as functions of the intermediate-level parameters.

In this hierarchical design methodology, two statistical characterizations are performed. First, the statistical distributions of the intermediate-level parameters are calculated from those of the low-level parameters. Second, the statistical distributions of the high-level circuit performances are calculated from the intermediate-level parameters. The first characterization can be quickly performed with the non-Monte Carlo techniques described in this paper. The second characterization can be performed either in the same way or using Monte Carlo analysis. Monte Carlo analysis is generally acceptable for the second characterization if the behavioral model being used is fast and involves only a relatively small

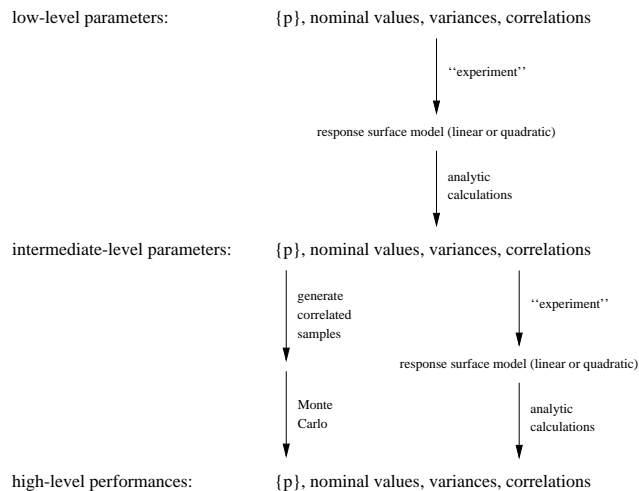


Figure 1: Hierarchical characterization.

number of statistical parameters, which is often the case.

The non-Monte Carlo techniques described in this paper utilize response surface methodology (RSM) [6]. RSM involves constructing a circuit model which is locally linear or quadratic in the statistical parameters. The RSM model is constructed by performing an “experiment” in which the lower-level parameters are permuted in a regular fashion about their nominal values. For each permutation of the lower-level parameters, a simulation is performed and the resultant values of the higher-level parameters are recorded. The coefficients of the RSM model are then obtained by linear regression. SIMPILOT [7] is a commercial tool which implements RSM.

At each level of the statistical characterization it is essential to consider the *correlations* between parameters, as independent parameters are uncommon. Computing and using a variance-covariance matrix of the parameters at each level of the hierarchy can properly account for parameter correlations and, furthermore, provides an excellent conduit for incorporating parameter mismatch information into circuit models. These variance-covariance matrices are one of the most important cornerstones of our methodology.

With these factors in mind, a typical flow of our statistical characterization process begins with a set of low-level process parameters, their nominal values, their variances, and their correlations. We construct an experiment and carry out simulations to build the quadratic response surface models for each component in the circuit. We use analytic formulas to calculate the means, vari-

	$M1_{pc1}$	$M1_{pc2}$	$M2_{pc1}$	$M2_{pc2}$	C_1	C_2
$M1_{pc1}$	1	0	0.9	0	0	0
$M1_{pc2}$	0	1	0	0.9	0	0
$M2_{pc1}$	0.9	0	1	0	0	0
$M2_{pc2}$	0	0.9	0	1	0	0
C_1	0	0	0	0	1	0.8
C_2	0	0	0	0	0.8	1

Figure 2: Example variance-covariance matrix for low-level parameters.

ances, and correlations of the intermediate-level parameters. We then perform Monte Carlo analysis at the behavioral level, using correlated sets of random variables, to determine the distributions and correlations of the high-level system performances.

Our key new contributions to this method of hierarchical statistical characterization, as shown in Figure 1, are in three areas:

1. a method for incorporating parameter mismatch and correlation into the response surface models,
2. a method for directly calculating the expected values, variances, and correlations of higher-level parameters from those of lower-level parameters, and
3. a method for generating correlated sets of parameters for Monte Carlo analysis at the behavioral level.

These contributions improve the efficiency and accuracy of statistical circuit characterization.

2 Parameter Mismatch and Correlation

Most MOS models are parameterized by a relatively large number of parameters, only a few of which are statistically independent [8]. *Principal component analysis* (PCA) or *principal factor analysis* (PFA) can be used to extract the statistically relevant combinations of parameters and thereby reduce the number of lower-level parameters which must be considered [9, 10]. Given a set of model cards which have been extracted from fabricated devices, SPAYN [11] is a commercial tool which performs PCA and PFA. This technique typically results in 2-3 statistically relevant principal components per transistor, which can explain at least 75% of the observed variation in 15 level 3 MOS model parameters.

In order to properly account for parameter mismatch, we use a separate model card for each transistor in the circuit. Correlations between transistors are specified in the variance-covariance matrix. The correlation coefficients will be functions of transistor areas, distances between transistors, and V_{gs} , according to appropriate mismatch models. Parameters on the same die will typically have relatively high correlation coefficients, approaching the limiting case of 1 for no mismatch. Note that using a single model card for multiple transistors, while common, corresponds to this limiting case of no mismatch and can produce inaccurate statistical characterizations. An example variance-covariance matrix is shown in Figure 2. In this example, there are two orthogonal principal factors for each transistor. There are two transistors whose parameters are 90% correlated. There are two capacitors which are 80% correlated to each other and uncorrelated to the transistor parameters.

3 Analytic Statistical Calculations

Once an appropriate variance-covariance matrix for the statistically-relevant low-level parameters has been obtained, we use SIMPILOT or a similar program to construct the linear or quadratic response surface models for each intermediate-level parameter. Constructing this model involves defining an appropriate experiment, which in SIMPILOT is typically a simplex experiment for linear models or a Latin hypercube for quadratic models, running ELDO [12] (SPICE) for each permutation in the experiment, and using linear regression to solve for the coefficients of the response surface model.

Once a linear or quadratic response surface model has been found, the expected values, variances, and correlations of the intermediate-level parameters can be directly computed, regardless of the distributions of the low-level parameters. Therefore it is usually not necessary to resort to Monte Carlo analysis, as SIMPILOT does; direct analytic solutions are faster and more accurate.

Let X be a p -dimensional vector of random variables which represents the lower-level parameters, with $\mathcal{E}[X] = \theta$ and variance-covariance matrix $\mathcal{D}[X] = \Sigma$. Let Y be an n -dimensional vector representing the higher-level parameters. We wish to calculate $\mathcal{E}[Y]$ and $\mathcal{D}[Y]$.

Considering the linear case first, let C be an $n \times p$ matrix of constants representing the statistically significant coefficients in the linear model, so that $Y = CX$. Theorems 3.1 and 3.2 prove that $\mathcal{E}[Y] = C\theta$ and $\mathcal{D}[Y] = C\Sigma C'$, respectively. Note that these theorems do not make any assumptions about the distribution of the low-level parameters X .

Theorem 3.1

$$\mathcal{E}[CX] = C\theta \quad (1)$$

Proof: Let $Y = CX$. Then $y_i = \sum_{r=1}^m c_{ir}x_r$, and

$$\mathcal{E}[CX] = [E[y_i]_i] \quad (2)$$

$$= \left[\left(\sum_{r=1}^m c_{ir} \mathcal{E}[x_r] \right)_i \right] \quad (3)$$

$$= [C\mathcal{E}[X]_i] \quad (4)$$

$$= C\theta \quad (5)$$

Theorem 3.2

$$\mathcal{D}[CX] = C\Sigma C' \quad (6)$$

Proof: Let $Y = CX$. Then

$$\mathcal{D}[CX] = \mathcal{D}[Y] \quad (7)$$

$$= \mathcal{E}[(Y - \mathcal{E}[Y])(Y - \mathcal{E}[Y])'] \quad (8)$$

$$= \mathcal{E}[(CX - C\mathcal{E}[X])(CX - C\mathcal{E}[X])'] \quad (9)$$

$$= \mathcal{E}[C(X - \mathcal{E}[X])(X - \mathcal{E}[X])'C'] \quad (10)$$

$$= C\mathcal{E}[(X - \mathcal{E}[X])(X - \mathcal{E}[X])']C' \quad (11)$$

$$= C\Sigma C' \quad (12)$$

For the quadratic case, let A be a $p \times p$ symmetric matrix representing the statistically significant coefficients in the quadratic model for any one higher-level parameter y_i , so that $y_i = X'AX$. Note that for any given coefficients in a quadratic equation, A is uniquely determined [13]. Let $tr(A)$ denote the trace of A . Theorems 3.3 and 3.4 show how $\mathcal{E}[y_i]$ and $var[y_i]$ can be calculated.

Theorem 3.3

$$\mathcal{E}(X'AX) = tr(A\Sigma) + \theta'A\theta \quad (13)$$

Proof:

$$\mathcal{E}[X'AX] = \mathcal{E}[(X - \theta)'A(X - \theta) + \theta'AX + X'A\theta - \theta'A\theta] \quad (14)$$

Since $X'A\theta = (X'A\theta)' = \theta'A'X = \theta'AX$

and $\mathcal{E}[\theta'AX] = \theta'A\mathcal{E}[X] = \theta'A\theta$,

$$\mathcal{E}[X'AX] = \mathcal{E}[(X - \theta)'A(X - \theta)] + \theta'A\theta \quad (15)$$

$$= \sum_i \sum_j a_{ij} \mathcal{E}[(x_i - \theta_i)(x_j - \theta_j)] + \theta'A\theta$$

$$= \sum_i \sum_j a_{ij} \sigma_{ij} + \theta'A\theta \quad (16)$$

$$= tr[A\Sigma] + \theta'A\theta \quad (17)$$

Theorem 3.4

$$\begin{aligned} \text{var} [X'AX] &= \mathcal{E} \left[((X - \theta)' A (X - \theta))^2 \right] + \\ &4\mathcal{E} \left[(\theta' A (X - \theta))^2 \right] + \\ &4\mathcal{E} \left[\theta' A (X - \theta) (X - \theta)' A (X - \theta) \right] - \\ &(\text{tr} (A\Sigma))^2 \end{aligned} \quad (18)$$

Proof:

$$\text{var} [X'AX] = \mathcal{E} \left[(X'AX)^2 \right] - (\mathcal{E} [X'AX])^2 \quad (19)$$

$$X'AX = (X - \theta)' A (X - \theta) + 2\theta' A (X - \theta) + \theta' A \theta \quad (20)$$

letting $W = X - \theta$,

$$\begin{aligned} (X'AX)^2 &= (W'AW)^2 + 4(\theta'AW)^2 + (\theta'A\theta)^2 + \\ &2\theta'A\theta(W'AW + 2\theta'AW) + \\ &4\theta'AWW'AW \end{aligned} \quad (21)$$

using 3.3,

$$\begin{aligned} \mathcal{E} \left[(X'AX)^2 \right] &= \mathcal{E} \left[(W'AW)^2 \right] + 4\mathcal{E} \left[(\theta'AW)^2 \right] + \\ &(\theta'A\theta)^2 + 2\theta'A\theta(\text{tr} (A\Sigma)) + \\ &4\mathcal{E} \left[\theta'AWW'AW \right] \end{aligned} \quad (22)$$

$$(\mathcal{E} [X'AX])^2 = (\text{tr} (A\Sigma))^2 + (\theta'A\theta)^2 + 2\theta'A\theta\text{tr} (A\Sigma) \quad (23)$$

$$\begin{aligned} \text{var} [X'AX] &= \mathcal{E} \left[(W'AW)^2 \right] + 4\mathcal{E} \left[(\theta'AW)^2 \right] + \\ &4\mathcal{E} \left[\theta'AWW'AW \right] - (\text{tr} (A\Sigma))^2 \end{aligned} \quad (24)$$

Evaluating (18) requires the second, third, and fourth moments of the joint probability density function for X and thus can be complicated in the general case. When X can be assumed to follow a multivariate normal distribution, i.e. $X \sim \mathcal{N}_p(\theta, \Sigma)$, then

$$\mathcal{E} \left[(W'AW)^2 \right] = (\text{tr} (A\Sigma))^2 + 2\text{tr} (A\Sigma)^2, \quad (25)$$

$$\mathcal{E} \left[(\theta'AW)^2 \right] = \theta' A \Sigma A \theta, \text{ and} \quad (26)$$

$$\mathcal{E} \left[\theta'AWW'AW \right] = 0. \quad (27)$$

Theorem 3.5 follows immediately [14].

Theorem 3.5 If $X \sim \mathcal{N}(\theta, \Sigma)$, then

$$\text{var} [X'AX] = 2\text{tr} (A\Sigma)^2 + 4\theta' A \Sigma A \theta \quad (28)$$

To compute the off-diagonal elements of $\mathcal{D}[Y]$, we need to compute $\text{cov} [y_i, y_j]$ for all i, j . Let A and B be the symmetric matrices representing the coefficients of the quadratic models for two higher-level parameters y_A and y_B , so that $y_A = X'AX$ and $y_B = X'BX$. Theorem 3.6 is used to compute $\text{cov} [y_i, y_j]$ [13].

Theorem 3.6 If $X \sim \mathcal{N}_p(\theta, \Sigma)$, then

$$\text{cov} (X'AX, X'BX) = 2\text{tr} (A\Sigma B\Sigma) + 4\theta' A \Sigma B \theta \quad (29)$$

Proof: Let $T = [X' \ X']$ be the $(2p)$ -dimensional vector formed by replicating X . $T \sim \mathcal{N}_{2p}(\mu, C)$, where $\mu = [\theta' \ \theta']$ and $C = \begin{bmatrix} \Sigma & \Sigma \\ \Sigma & \Sigma \end{bmatrix}$. Let $W = \begin{bmatrix} A & 0 \\ 0 & B \end{bmatrix}$. Then

$$T'WT = X'AX + X'BX \quad (30)$$

$$\begin{aligned} \text{var} [T'WT] &= \text{var} [X'AX] + \text{var} [X'BX] \\ &- 2\text{cov} [X'AX, X'BX] \end{aligned} \quad (31)$$

$$\begin{aligned} \text{cov} [X'AX, X'BX] &= \frac{1}{2} (2\text{tr} (WC)^2 + 4\mu'WCW\mu - \\ &(2\text{tr} (A\Sigma)^2 + 4\theta' A \Sigma A \theta) - \\ &(2\text{tr} (B\Sigma)^2 + 4\theta' B \Sigma B \theta)) \end{aligned} \quad (32)$$

$$= 2\text{tr} (A\Sigma B\Sigma) + 4\theta' A \Sigma B \theta \quad (33)$$

Our IC fabrication experience has shown that the low-level parameters generally *do* follow a normal or log-normal distribution, so normality of the low-level parameters, as required by Theorems 3.5 and 3.6, is a reasonable assumption. One frequently-cited theoretical justification for this assumption is the central limit theorem applied to the physical fabrication process.

If the low-level parameters X can be assumed to be multivariate normal, $X \sim \mathcal{N}_p[\theta, \Sigma]$, and a linear model is used, then the intermediate-level parameters Y will also be multivariate normal, $Y \sim \mathcal{N}_n [C\theta, C\Sigma C']$. When X is multivariate normal and a quadratic model is used, then $(X - \theta)' A (X - \theta) \sim \chi_r^2$ if and only if $A\Sigma A = A$, where r is the rank of A [14]. Otherwise the distribution of Y does not follow an easily-computable form. In practice, however, one introduces little error by assuming that the intermediate parameters are approximately multivariate normal, even when a quadratic model is used.

Our C functions for calculating the expected values and variance-covariance matrix using (1), (6), (13), (28), and (29) accept as inputs the vector θ and the matrix Σ , which define the joint distributions of the low-level parameters, and a coefficient matrix C in which each row represents the appropriately-ordered response surface coefficients for one intermediate-level parameter. For example, if the response surface models for two intermediate-level parameters, p_0 and p_1 , are

$$p_0 = c_{00} + c_{01}x_1 + c_{02}x_1^2 + c_{03}x_2 + c_{04}x_2x_1 + c_{05}x_2^2 \quad (34)$$

and

$$p_1 = c_{10} + c_{11}x_1 + c_{12}x_1^2 + c_{13}x_2 + c_{14}x_2x_1 + c_{15}x_2^2 \quad (35)$$

then

$$C = \begin{bmatrix} c_{00} & c_{01} & c_{02} & c_{03} & c_{04} & c_{05} \\ c_{10} & c_{11} & c_{12} & c_{13} & c_{14} & c_{15} \end{bmatrix} \quad (36)$$

The C functions for the linear case are straightforward. For the quadratic case, the expected value function loops over each intermediate-level parameter, calling (13) to compute the expected value of that parameter. Similarly, the variance-covariance function loops over each combination of intermediate-level parameters, calling (28) or (29) to compute the appropriate entry in the variance-covariance matrix for that combination. A utility function converts a row of the matrix C into a symmetric matrix of the appropriate form to be used as A or B .

4 Correlated Parameters at the Behavioral Level

Using the techniques outlined in Sections 2 and 3 we can calculate the nominal values, variances, and correlations of the intermediate-level parameters. If there are a large number of correlated intermediate-level parameters, then PFA or PCA can be used again, in the same fashion as for the low-level parameters, to reduce the number of parameters which must be considered for the behavioral modeling. Given the distributions of the intermediate-level parameters, the next step is to calculate the distributions of the high-level performances. We can either repeat the RSM-based procedure used to characterize the intermediate-level parameters or we can perform a Monte Carlo simulation. Monte Carlo simulations at the behavioral level are feasible if there are a relatively

```

for  $i = 1$  to  $p$  {
   $\sigma_{ii} = \sqrt{\sigma_{ii} - \sum_{k=1}^{i-1} \sigma_{ki}^2}$ 
  for  $j = i + 1$  to  $p$  {
     $\sigma_{ij} = \frac{\sigma_{ij} - \sum_{k=1}^{i-1} \sigma_{ki} \sigma_{kj}}{\sigma_{ii}}$ 
  }
}

```

Figure 3: Pseudo-code for computing the Cholesky decomposition of Σ .

small number of intermediate-level parameters and each evaluation of the behavioral model is fast.

When performing these behavioral-level Monte Carlo simulations, it is essential that the correlations between the intermediate-level parameters be properly considered; treating them as independent will usually produce overly pessimistic results. The way to do this is to generate *correlated* sets of random numbers. Suppose we want a $p \times 1$ vector of random variables to be correlated, with variance-covariance matrix Σ . We can form the Cholesky decomposition of Σ to obtain an upper triangular matrix U , where

$$\Sigma = U^T U \quad (37)$$

If we generate a $p \times 1$ vector of independent random variables X , with $\mathcal{E}[X] = 0$ and $\mathcal{D}[X] = I$, then $U^T X$ will have $\mathcal{E}[U^T X] = 0$ and $\mathcal{D}[U^T X] = \Sigma$. Therefore pre-multiplying X by U^T induces the desired correlations.

Pseudo-code for computing the Cholesky decomposition of a symmetric positive semidefinite $p \times p$ matrix Σ is shown in Figure 3. Note that all variance-covariance matrices are symmetric and positive semidefinite [14].

5 Results

The statistical characterization techniques described in this paper have been tested by performing statistical characterizations of two circuits. The first circuit is a folded cascode operational amplifier, which illustrates the building of a statistical behavioral model from a SPICE-level block. The second circuit is a phase-locked loop, which illustrates our complete methodology using multiple levels of hierarchy.

5.1 Folded Cascode Operational Amplifier

A transistor-level schematic of the folded cascode operational amplifier is shown in Figure 4. We statistically characterized five intermediate-level parameters: gain, pole₁, pole₂, r_{in} , and zero₁. These quantities represent the parameters which might be needed for a behavioral model of this operational amplifier.

For the statistical MOS models we used the example database distributed with SPAYN, which contains level 3 parameters for both p- and n-type transistors. Since no mismatch data was available, we assumed perfect transistor parameter matching (correlation = 1).

The statistically relevant transistor parameters were found using PCA in SPAYN to be n_{pc1} and n_{pc2} for the n-type transistors and p_{pc1} and p_{pc2} for the p-type. Considering also the variations in load capacitors and DC voltage sources, the complete set of low-level parameters for this example was $\{n_{pc1}, n_{pc2}, p_{pc1}, p_{pc2}, c_1, c_2, v_1, v_2\}$.

The intermediate-level parameters were defined to be $\{\text{gain}, \text{pole}_1, \text{pole}_2, r_{in}, \text{zero}_1\}$. Offset would have also been included as an intermediate-level parameter if transistor parameter correlation (mismatch) information had been available. The linear and quadratic response surface models for these intermediate-level parameters were found using SIMPILOT. Using these models, the

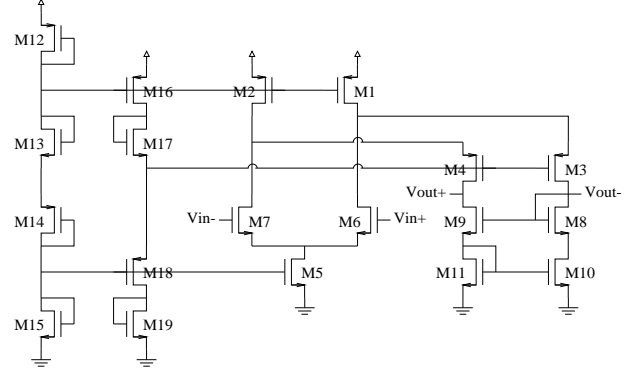


Figure 4: Transistor-level schematic of operational amplifier circuit.

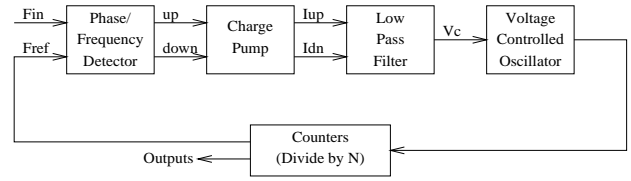


Figure 5: Block diagram of PLL.

appropriate functions from Section 3 were used to compute the expected values, standard deviations, and variance-covariance matrix of the intermediate-level parameters. The results of these analytic calculations and the CPU times on a DEC 7000 Model 610 AXP workstation are shown in Table 1.

For comparison to these analytic results, a 1,000-run Monte Carlo analysis was performed on the same circuit. The resultant expected values, standard deviations, and CPU time are also shown in Table 1. Note that the Monte Carlo results match the analytic results quite closely.

Correlated samples of these intermediate-level parameters were generated by computing the Cholesky decomposition U of the variance-covariance matrix found for the quadratic models, as discussed in Section 4. These correlated samples can be used in behavioral-level Monte Carlo analysis when this operational amplifier is included in larger systems.

5.2 Phase-Locked Loop

A block diagram of a commercially available PLL which is used as a clock multiplier and for deskewing is shown in Figure 5. The phase/frequency detector compares the phase and frequency of the input signal to the reference signal. If the frequency of the reference signal needs to be increased, then the signal *up* is asserted and the charge pump adds charge to the node V_c . Similarly, if the frequency of the reference signal needs to be decreased, then the signal *down* is asserted and the charge pump subtracts charge from the node V_c . The voltage controlled oscillator generates a frequency corresponding to the voltage on node V_c ; when the PLL is locked, the frequency generated by the oscillator is 12 times the input frequency.

The high-level performance which we wish to statistically characterize is the lock time, which we define as the time after which V_c lies in a band that is within 1.5% of its average value for the next 1 μ s. Calculating the lock time of the PLL using a transistor-level netlist requires more than 24 hours of CPU time on a Sun Ultra Sparc workstation, so traditional Monte Carlo methods would require thousands of days of CPU time and hence are impractical.

The intermediate-level parameters for the behavioral model of the voltage controlled oscillator are

Parameter	Linear Model		Quadratic Model		Monte Carlo Analysis	
	Nominal	St. Dev.	Nominal	St. Dev.	Nominal	St. Dev.
gain	110.2 dB	2.001 dB	110.2 dB	2.086 dB	110.2 dB	2.000 dB
pole ₁	902.0 Hz	310.1 Hz	911.4 Hz	336.5 Hz	917.2 Hz	347.2 Hz
pole ₂	4.025 MHz	0.763 MHz	4.028 MHz	0.766 MHz	4.026 MHz	0.783 MHz
r _{in}	414.2 GΩ	19.73 GΩ	414.5 GΩ	20.34 GΩ	413.9 GΩ	19.88 GΩ
zero ₁	3.971 MHz	0.752 MHz	3.973 MHz	0.754 MHz	3.971 MHz	0.770 MHz
CPU time	24.1 s		120.5 s		2258.6 s	

Table 1: Expected values and standard deviations of intermediate-level parameters.

Component	Distribution
PC1	log normal
PC2	log normal
PC3	Gaussian
PC4	Gaussian
PC5	negative log normal
PC6	Gaussian
PC7	negative log normal
PC8	Gaussian

Table 2: Distributions of principal components of MOS models.

1. gain, in MHz/V, and
2. $f_{0.8}$, the output frequency when $V_c = 0.8$ V.

The intermediate-level parameters for the behavioral model of the phase/frequency detector and charge pump are

1. I_{up} and
2. I_{dn} .

The behavioral models are written in HDLA [15].

5.2.1 MOS Model Extraction

Statistical MOS models are needed to characterize the blocks in the PLL. To obtain these models, we measured a sample of 100 dies from 5 wafers and 2 lots of a 0.5 μm double poly 3.3 V technology. Each die contained 5 NMOS and 5 PMOS transistors with W/L dimensions of 10 $\mu\text{m}/0.5 \mu\text{m}$, 10 $\mu\text{m}/0.4 \mu\text{m}$, 2 $\mu\text{m}/10 \mu\text{m}$, 0.8 $\mu\text{m}/10 \mu\text{m}$, and 10 $\mu\text{m}/10 \mu\text{m}$. SGS-Thomson Level 3 NMOS and PMOS models were extracted for each die, with 28 parameters per model. The accuracy of the models is within 5%. An example of extraction is shown in Figure 6.

The total measurement time was 45 hours using UTMOST [16] and a prober driven by a Sun Sparc 10. Extracting the models from the measurements took 25 hours of CPU time on a Sun Sparc 20. The extracted models for 7 of the 100 dies were grossly inaccurate; those dies were discarded.

The model cards were analyzed using principal component analysis and 8 statistically significant principal components were found. Three distributions were considered for each principal component: Gaussian, log normal, and negative log normal. Note that a log normal distribution is the distribution of $y = e^x$ when x is Gaussian and a negative log normal is the distribution of $z = t - y$ where t is any real number. For each principal component, the distribution which produces the best fit is chosen. The resultant distributions are shown in Table 2 and a histogram of principal component 7 is shown in Figure 7. Regardless of distribution, each principal component is standardized to have mean = 0 and standard deviation = 1.

5.2.2 Behavioral Model Parameters

Given the statistical transistor models, the next step is to compute the distributions of the intermediate-level behavioral model pa-

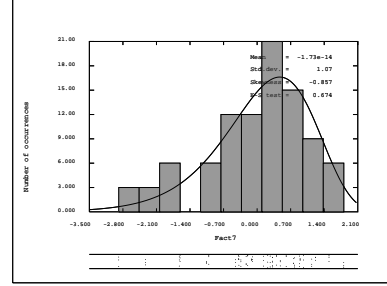


Figure 7: Histogram of principal component 7 of MOS models.

Parameter	Linear Model		Quadratic Model	
	Accuracy	Worst Error	Accuracy	Worst Error
gain	92.46%	2.39%	92.60%	-1.87%
$f_{0.8}$	77.53%	-13.07%	81.48%	-10.33%
I_{up}	74.18%	-7.35%	78.15%	-4.31%
I_{dn}	73.28%	-7.39%	77.42%	-4.35%

Table 3: Comparison of linear and quadratic models for intermediate-level parameters.

rameters. We begin by building the linear and quadratic response surface models of the intermediate-level parameters as functions of the principal components of the MOS models.

To calculate the voltage controlled oscillator parameters, gain and $f_{0.8}$, we ran transient simulations at four input voltages, measuring the frequency as the average frequency of the last 25 of 120 periods at each input voltage. Gain is calculated as the slope of the least squares estimate of the straight-line function of frequency as a function of input voltage. $F_{0.8}$ is the frequency when the input is at 0.8 V. The accuracies of the linear and quadratic models for gain and $f_{0.8}$ are shown in Table 3. The CPU times required to build these models are summarized in Table 4.

The phase/frequency detector and charge pump parameters, I_{up} and I_{dn} , were measured by applying the input and reference frequencies for 200 μs and averaging the I_{up} and I_{dn} signals over the period (20 μs , 180 μs). The accuracies of the linear and quadratic models for I_{up} and I_{dn} are shown in Table 3, and the CPU times are summarized in Table 4.

We note that the linear models are almost as accurate as the quadratic models, so we use the linear models for the statistical calculations.

Since not all of the principal components of the MOS models were Gaussian, we computed the statistical distributions of the intermediate-level parameters in two different ways. The first method was the theoretical approach, using Equations 1 and 6. The second method was a 10,000-run Monte Carlo analysis using the linear RSM model. The results are summarized in Table 5; it is

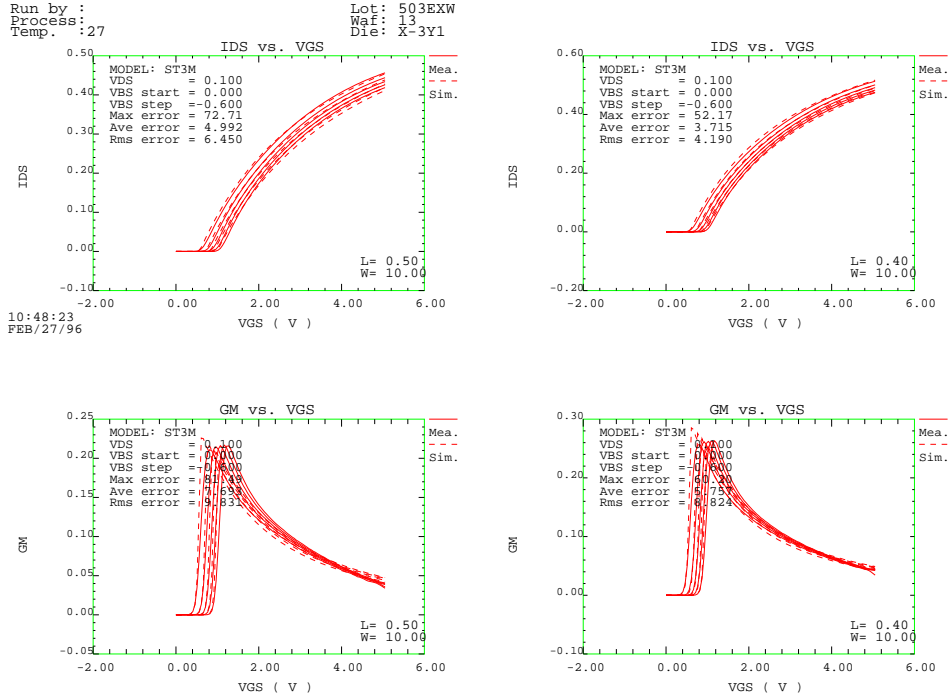


Figure 6: Extraction using UTMOST.

Parameters	Linear Model	Quadratic Model
gain and $f_{0.8}$	7.50 hours	68.0 hours
I_{up} and I_{dn}	4.26 hours	38.4 hours
total:	11.76 hours	106.4 hours

	gain	$f_{0.8}$	I_{up}	I_{dn}
gain	1.000	0.579	0.881	0.880
$f_{0.8}$	0.579	1.000	0.670	0.671
I_{up}	0.881	0.670	1.000	0.99999
I_{dn}	0.880	0.671	0.99999	1.000

Table 4: CPU times for building linear and quadratic models of intermediate-level parameters, on a Sun Sparc 20.

Figure 9: Matrix of correlation coefficients of intermediate-level parameters.

Parameter	Analytic Calculations		RSM Monte Carlo	
	Nominal	St. Dev.	Nominal	St. Dev.
gain	172.3 MHz/V	2.38%	170.9 MHz/V	2.45%
$f_{0.8}$	38.71 MHz	4.03%	37.34 MHz	4.15%
I_{up}	191.1 μ A	2.21%	190.8 μ A	2.22%
I_{dn}	191.1 μ A	2.20%	190.4 μ A	2.16%

Table 5: Expected values and standard deviations of intermediate-level parameters.

Parameter	Linear Model		Quadratic Model	
	Accuracy	Worst Error	Accuracy	Worst Error
lock time	50.68%	-3.27%	92.53%	-0.93%

Table 6: Comparison of linear and quadratic models for high-level performance.

clear that the analytic method and the RSM Monte Carlo method produce almost identical results. The actual distributions obtained from the Monte Carlo analyses are shown in Figure 8. The matrix of the correlation coefficients of the intermediate-level parameters is shown in Figure 9.

5.2.3 High-Level Performance

Once the statistical distributions of the intermediate-level behavioral model parameters have been found, we can compute the distribution of the high-level performance in which we are interested, the lock time of the PLL.

Figure 9 shows that I_{up} and I_{dn} are very highly correlated and

Parameter	Analytic Calculations		RSM Monte Carlo	
	Nominal	St. Dev.	Nominal	St. Dev.
lock time	7.1642 μ s	1.21%	7.1643 μ s	1.16%

Table 7: Expected values and standard deviations of high-level performance.

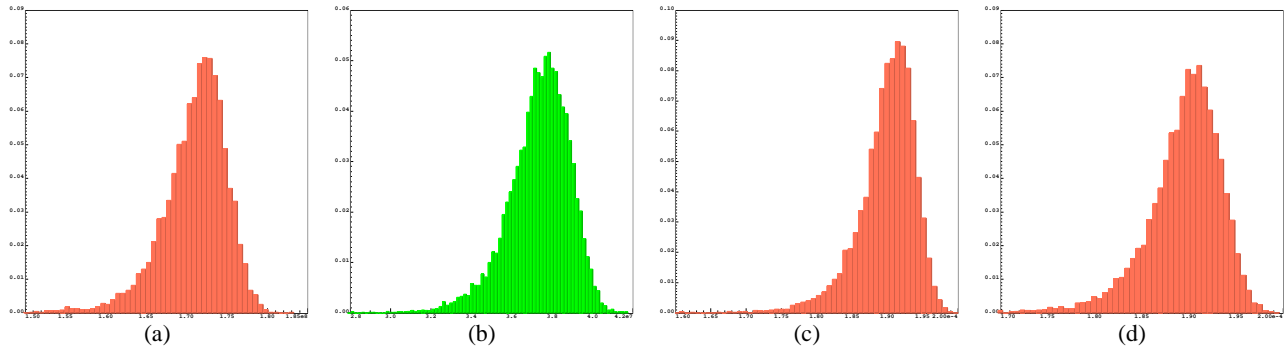


Figure 8: Histograms of (a) gain, (b) $f_{0.8}$, (c) I_{up} , and (d) I_{dn} .

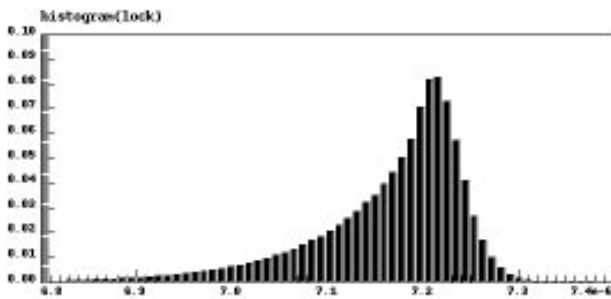


Figure 10: Distribution of lock time.

that gain is highly correlated to I_{up} and I_{dn} . We therefore attempt a parameter reduction by performing a principal component analysis on the intermediate-level parameters. Only the first two principal components turn out to be statistically significant, and together they explain 96.22% of the parameter variation.

Next we build the linear and quadratic RSM models of the lock time as a function of PC1 and PC2, the first two principal components of the intermediate-level parameters. The relative accuracy of these models is shown in Table 6. Since the quadratic model is significantly more accurate than the linear model, the quadratic model is used for the statistical calculations.

We compute the statistical distribution of the lock time by both the analytic method and the RSM Monte Carlo method (1,000,000-run sample). The results are shown in Table 7. The distribution of the lock time, as computed from the RSM Monte Carlo analysis, is shown in Figure 10.

6 Conclusions

We have developed a complete methodology for hierarchical statistical circuit characterization which does not rely upon circuit-level Monte Carlo simulation. The main new ideas are (1) a method for incorporating parameter mismatch and correlation into RSM, (2) a method for directly calculating expected values, variances, and correlations of higher-level parameters from those of lower-level parameters, and (3) a method for generating correlated sets of parameters for Monte Carlo analysis at the behavioral level. We have illustrated these ideas on two example circuits, a folded cascode operational amplifier and a phase-locked loop.

One main area of future work is in determining appropriate correlation coefficients to accurately model mismatch; in our example circuits we had to assume perfect matching.

We believe this methodology will be useful for yield analysis, setting realistic circuit specifications for large analog circuits, real-

istic worst-case modeling for both analog and digital circuits, enforcing matching constraints in constraint-driven place and route, and top-down constraint-driven design.

References

- [1] J.M. Hammersley and D.C. Handscomb, *Monte Carlo Methods*, London, Methuen & Co Ltd., 1964.
- [2] R.Y. Rubinstein, *Simulation and the Monte Carlo Method*, John Wiley & Sons, 1981.
- [3] H. Chang, A. Sangiovanni-Vincentelli, E. Charbon, U. Choudhury, E. Felt, G. Jusuf, E. Liu, E. Malavasi and R. Neff, "A Top-Down, Constraint-Driven Design Methodology for Analog Integrated Circuits", in *Proc. Workshop on "Advances in Analog Circuit Design," Scheveningen, NL*, pp. 301–325, April 1992.
- [4] B. Johnson, T. Quarles, A.R. Newton, D.O. Pederson and A. Sangiovanni-Vincentelli, *SPICE3 Version 3f User's Manual*, University of California, Berkeley, 1992.
- [5] L.A. Williams and B.A. Wooley, "MIDAS—A Functional Simulator for Mixed Digital and Analog Sampled Data Systems", *Proc. IEEE International Symposium on Circuits and Systems*, vol. 5, pp. 2148–2151, 1992.
- [6] R.H. Myers and D.C. Montgomery, *Response Surface Methodology: Process and Product Optimization Using Designed Experiments*, John Wiley & Sons, New York, 1995.
- [7] ANACAD Electrical Engineering Software, *SimPilot User's Manual*, ULM (Donau) Germany, 1995.
- [8] P. Yang, D. Hocevar, P. Cox, C. Machala and P. Chatterjee, "An integrated and efficient approach for MOS VLSI statistical circuit design", in *IEEE Trans. on Computer-Aided Design of Integrated Circuits and Systems*, volume CAD-5, pp. 5–14, January 1986.
- [9] T.D. Wickens, *The Geometry of Multivariate Statistics*, Lawrence Erlbaum Associates, Hillsdale, New Jersey, 1995.
- [10] J.E. Jackson, *A User's Guide to Principal Components*, John Wiley & Sons, New York, 1991.
- [11] Silvaco International, *SPAYN User's Manual*, Santa Clara, California, 1995.
- [12] ANACAD Electrical Engineering Software, *ELDO User's Manual*, ULM (Donau) Germany, 1995.
- [13] S.R. Searle, *Linear Models*, John Wiley & Sons, New York, 1971.
- [14] G.A.F. Seber, *Linear Regression Analysis*, John Wiley & Sons, New York, 1977.
- [15] ANACAD Electrical Engineering Software, *HDLA User's Manual*, ULM (Donau) Germany, 1995.
- [16] Silvaco International, *UTMOST User's Manual*, Santa Clara, California, 1995.